International Journal of Engineering and Technology Innovation, vol. 8, no. 3, 2018, pp. 228-239

On the Mechanism Design of an Innovative Elliptical Exerciser with Quick-Return Effect

Fu-Chen Chen[1,*], Yih-Fong Tzeng[2], Wei-Ren Chen[1]

[1]Department of Mechanical Engineering, Kun Shan University, Tainan, Taiwan, ROC

[2]Department of Mechanical and Automation Engineering, National Kaohsiung University of Science and Technology, Yenchao, Kaohsiung, Taiwan, ROC

Received 22 April 2018; received in revised form 23 May 2018; accepted 10 June 2016

Abstract

The objective of this study is to propose and investigate an innovative elliptical exerciser with quick-return effect that mimics the timing of the foot trajectory while jogging. At first, the innovative mechanism of the elliptical exerciser with quick-return effect is proposed. The structure and function of the proposed design are introduced. Then, the mechanism is analysed kinematically using the vector-loop method and motion geometry of the mechanism. An illustration is presented for explaining the design procedure of the proposed innovative design. Finally, the pedal trajectory of the innovative elliptical exerciser is simulated. The simulation results validate that the motion of pedal trajectory on the striding travel is faster than that on the supporting travel. Because of this quick-return effect, the timing of the pedal trajectory meets the principles of ergonomics and prevents the user suffering from muscle sore, pain or even injury.

Keywords: mechanism design, quick-return mechanism, elliptical exerciser

1. Introduction

An apparatus that transforms rotary motion into reciprocating motion and provides a slow forward stroke and a quick return stroke is called a quick return mechanism. It can be seen in every corner of the mechanical industry across various machines such as shaper, stamping press, power-driven reciprocating saw, mechanical actuator and so on. Crank-shaper mechanism, Whitworth mechanism, offset crank-slider mechanism, and drag-link mechanism are quick return mechanisms. They are popular and can be found in the literature [1-2]. Quick return mechanisms are used in machine tools for the purpose of offering the reciprocating cutting tool a slow cutting stroke and a quick return stroke at a constant angular speed of the driving crank. The ratio of time required for the slow cutting stroke to the time required for the quick return stroke is called the time ratio (TR) and is greater than one [2]. The mechanism usually consists of a connecting link adjacent to a rotary flywheel that rotates at a constant angular velocity. The connecting link of the mechanism operates at a different velocity from the flywheel. Because the flywheel operates at a different speed from the connecting link, the efficiency is increased when the amount of time required for a cut is reduced. From the mechanical engineering viewpoint, the technology of the Industrial Revolution is promoted by the quick return mechanisms through minimizing the time of a full revolution, thus reducing the amount of time required for a cut or press.

The research about quick return mechanisms can be found in a lot of literatures. Dwivedi [3] modified the Whitworth quick return mechanism to construct high-velocity impacting press. This machine includes a Whitworth quick return mechanism

* Corresponding author. E-mail address: fcchen@mail.ksu.edu.tw

composed of a crank and a drive arm together with a variable speed D.C. motor, a flywheel, bearings, etc. Besides, this study investigates the causes of the unbalanced forces and methods to depress the loads delivered to the frame of this machine. Sua reo & Gupta [4] used an algebraic method to synthesize quick-returning RSSR mechanisms that meet the given time-ratio and the requirement of the follower oscillation angle. Beale and Scott [5] used Galerkin's approach to study the response and stability of a flexible rod in the quick return mechanism.

Fung et al [6-8] derived the governing equation of a quick return mechanism by way of using the finite element method (FEM) with time-dependent parameter and Hamilton's principle. Lin and Wai [9-10] proposed a control approach based on fuzzy neural network to investigate its dynamic response of a quick return mechanism. Ha et al [11] proposed the use of finite difference method (FDM) with constant and variable grids to approach the numerical solutions of a flexible quick-return mechanism. Chang [12] studied the rotor-mechanism coupling effect and found that the dynamic behaviors of the coupled system are not identical to those uncoupled systems. Hsieh and Tsai [13] invented a novel design of quick return mechanism that is composed of a generalized Oldham coupling and a slider-crank mechanism. The proposed design is more compact than a traditional design and can be balanced easily.

Jogging is a popular exercise. It is known that the jogger's knees suffer from significant impact especially at the moment that the foot hits the ground. The knees could be easily injured after constantly taking the impacts for a period of time. Therefore, many exercisers such as elliptical exercisers, stepper, and air walker are developed to guide the feet to move along a trajectory that is similar to that of real jogging, only that the knees are well protected from being impacted and injured.

A conventional elliptical exerciser comprises a frame, two handles, a flywheel and two foot support members. Both the flywheel and the handles connect with the frame, and one end of the foot support member connects to the flywheel and the other end to the handle. When the handles swing, the foot support members are driven by the flywheel and moved along a pedal trajectory that comprises a supporting travel and a striding travel.

However, the pedal trajectory provided by the conventional elliptical exerciser is an elliptical trajectory, and the pedals traveling on two sides of the flywheel are separated with 180 degrees of phase angle. When using the conventional elliptical exercisers, the user has to make his gait cooperate with the pedal trajectory constrained by the elliptical exerciser, so that the user cannot shift his weight from one leg to the other until his two legs reach their respective extreme positions. The accumulation of the muscles sore and pain may cause sports injury to the user, and even worse if the user does not tread the pedals at a suitable angle. Besides, the timing of pedal trajectory by the conventional elliptical exerciser is quite different from what in the real jogging.

The foot support links connecting with the flywheel on two sides of the conventional elliptical exercisers have 180 degrees of phase difference, so that when one of the user's feet is at the front end of a pedal trajectory and going to support the user's weight, the other one is at the rear end of the pedal trajectory. As shown in Fig. 1(a), the supporting travel **A1** and the striding travel **A2** of the pedal trajectory **A** have almost the same path length. However, in real jogging, when one of the user's feet is at the front end of the trajectory and begins to support the user's weight, the other one has not yet reached the rear end of the trajectory but still on the way of its backward path. In fact, it could not begin to move forward until it reaches the rear end of the trajectory. As shown in Fig. 1(b), in the trajectory B of real jogging, the path length of the supporting travel **B1** should be less than that of the striding travel **B2**. The conventional elliptical exerciser cannot provide the user with the real jogging exercising timing and does not meet the principles of ergonomics.

Copyright © TAETI

There are a lot of patents about elliptical exercisers, but little research studied the mechanism design of elliptical exercisers. Shyu et al [14] presented an innovative design of adjustable elliptical exerciser, in which stride and inclined angle are both adjustable. Even though a lot of various kinematic structures have been used in the make-up of elliptical trainer machines for exercise and fitness, none of them do give pedal trajectories that boost lower extremity kinematics similar to over ground stride. Nelson and Burnfield [15] presented an innovative design method for elliptical machines and tried to make a movement path that more closely mimics the lower extremity kinematics of gait. This novel design introduces a modified Cardan gear system in substitution for the typical crank link.

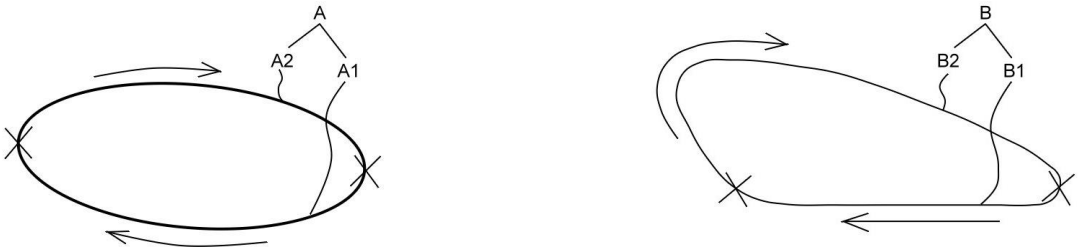

(a) Elliptical trajectory (b) Real trajectory

Fig. 1 Foot trajectory

Porcari et al [16-17] studied and compared the physiological responses of a new elliptical exercise machine (ELLIPSE) to standard exercise modalities such as treadmill running (TMrun), walking (TMwalk), stationary cycling (BIKE), and stepping (STEP). The conclusion indicated that TMrun and ELLIPS require a greater physiologic load compared with TMwalk, BIKE, or STEP. Because the vertical ground reaction force for the ELLIPSE was smaller than half of TMrun, it may result in a fewer risk of injury. Sozen [18] investigated and compared muscle activation during elliptical trainer, treadmill, and bike exercise. Louie and Lam [19] attempted to compare the physiological variables of two models of the elliptical trainer. Data of heart beat rate and energy expenditure was recorded. The results showed that users exercising on the latest elliptical model results in the higher heart-beat rate and consumes more energy.

The objective of this study is to propose an innovative elliptical exerciser that includes a quick-return mechanism. The innovative design allows that the pedal moves from the striding travel to the supporting travel before the other pedal reaches the rear end of the pedal trajectory. Therefore, the two legs do not need to stretch to their extreme positions when the user's weight is shifted from one leg to the other.

2. Innovative Elliptical Exerciser

The innovative elliptical exerciser proposed in this study is shown in Fig. 2. The design comprises a frame, a flywheel, two swing handles, two foot support links, two bell cranks and two connecting links. The bell crank is a lever having its fixed pivot at the apex of the angle formed by its two arms. The flywheel and the bell cranks rotate with respect to the frame in the same manner. One end of the bell crank connects with the foot support link and the other end with the connecting link. Each of the two connecting link connects with the flywheel and the bell crank. The joints between the flywheel and the two connecting links are in the opposite position. Therefore, when one of the foot support links moves within the supporting travel, the corresponding bell crank drives the respective connecting link to rotate the flywheel. Thus, the other connecting link and the other bell crank drive the other foot support link to move along the striding travel.

As one of the foot support links is pedaled downward by the user, the foot support link drives the bell crank to rotate clockwise about the fixed pivot. The foot support link is guided by the bell crank to move along the supporting travel, and the bell

Copyright © TAETI

crank drives the connecting link to rotate the flywheel clockwise about its pivot. During the supporting travel, the rotational speed of the bell crank (on the right side) is slower than that of the flywheel. The flywheel then drives the other bell crank (on the left side) by way of the other connecting link, such that the rotational speed of the other bell crank is faster than the fly wheel. The two bell cranks have different rotational speeds such that the speed of the other foot support link is faster while it moves within the striding travel.

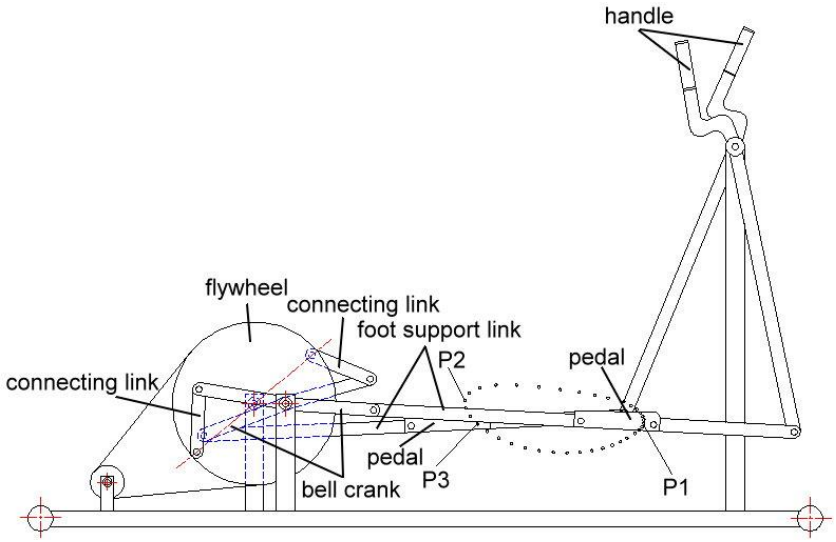

Fig. 2 Innovative elliptical exerciser

On the contrary, as shown in Fig. 3, when the other foot support link (on the left side) moves within the supporting travel, the rotary speed of the other bell crank is slower than the flywheel. The flywheel then drives the bell crank (on the right side) by way of the connecting link, such that the rotary speed of the bell crank is faster than the flywheel. By utilizing the quick-return effect to switch the speed of the two support links repeatedly, the two foot support links have different speeds when the two foot support links move within the supporting travel and within the striding travel. The motion mode generated by the proposed mechanism is more close to that in the real jogging.

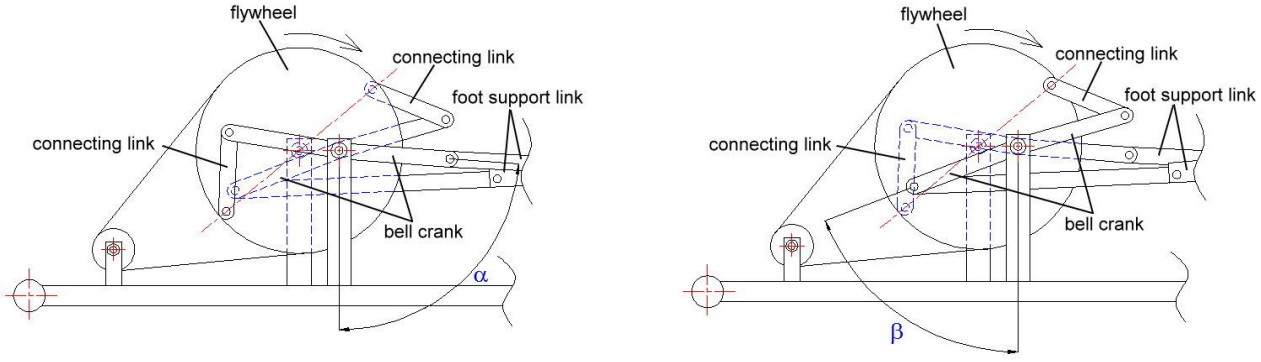

(a) Front position (b) Rear position

Fig. 3 Detail drawing of elliptical exerciser

In Figs. 2 and 3, the quick-return effect for producing speed difference is further illustrated as follows. When one of the foot support links moves within the supporting travel, the rotary speed of the bell crank is slower than that of the flywheel. Therefore, when the flywheel rotates clockwise 180 degrees, the bell crank has not rotated 180 degrees (i.e. the sum of the angle α in Fig. 3(a) and the angle β in Fig. 3(b) is less than 180 degrees). The pedal of the foot support link is at the point **P3** rather than the rear end **P2** of the trajectory at that time in Fig. 2. In other words, the user does not start to move his right foot from the point **P3** to the rear end **P2** of the pedal trajectory until his left foot on the other foot support link reaches at the front end **P1** of the supporting travel.

Copyright © TAETI

Therefore, the timing of the pedal trajectory in this innovative design is more similar to the one of real jogging and meets the principles of ergonomics. When using this proposed elliptical exerciser, the user can shift his body weight from one leg to the other before both of his legs stretch to their extreme positions. This motion pattern prevents the user suffering from muscle sore and pain.

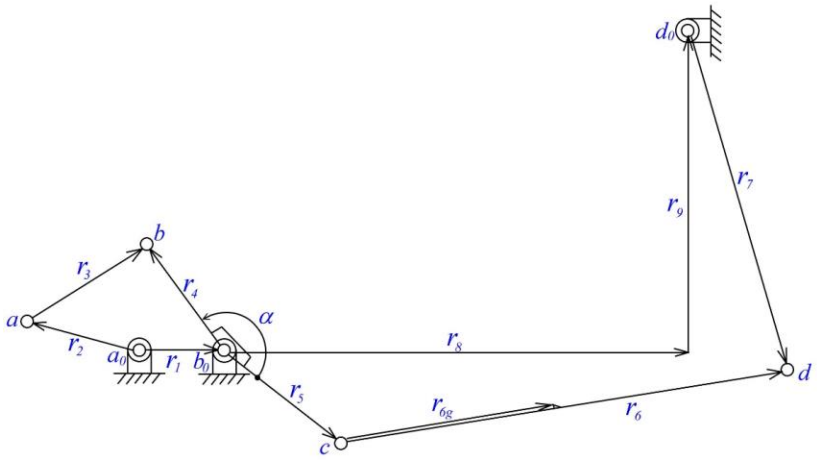

Fig. 4 Vector loop diagram

3. Motion Geometry

From the vector loop diagram of the innovative elliptical exerciser linkage assembly in Fig. 4, the following two vector loop equations can be derived as

$$\vec{r}_2 + \vec{r}_3 - \vec{r}_4 - \vec{r}_1 = 0 \tag{1}$$

$$\vec{r}_5 + \vec{r}_6 - \vec{r}_7 - \vec{r}_8 - \vec{r}_9 = 0 \tag{2}$$

By decomposing the vectors in Eq. (2) into *X* and *Y* scalar components, the equations become

$$r_5 \cos\theta_5 + r_6 \cos\theta_6 - r_7 \cos\theta_7 - r_8 = 0 \tag{3a}$$

$$r_5 \sin\theta_5 + r_6 \sin\theta_6 - r_7 \sin\theta_7 - r_9 = 0 \tag{3b}$$

When the foot support link is at the front end **P1** of the pedal trajectory in Fig. 2, vectors $\vec{r}_5$ and $\vec{r}_6$ are collinear (as shown in Fig. 5), i.e. $\theta_5 = \theta_6$. Rearranging Eqs. (3a) and (3b), it yields

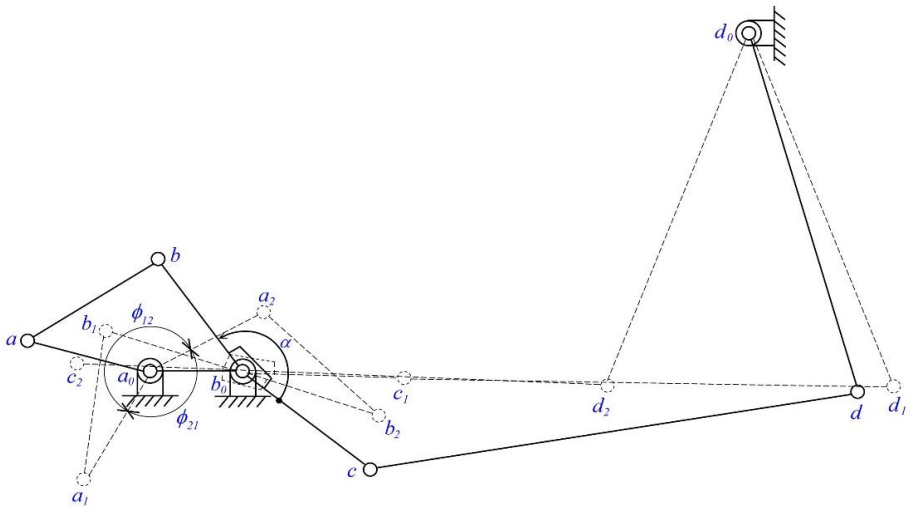

Fig. 5 Geometry at supporting and striding travels

Copyright © TAETI

$$(r_5 + r_6)\cos\theta_5 = r_7\cos\theta_7 + r_8 \tag{4a}$$

$$(r_5 + r_6)\sin\theta_5 = r_7\sin\theta_7 + r_9 \tag{4b}$$

Squaring Eqs. (4a) and (4b) and adding them together, it yields

$$A_1\cos\theta_7 + B_1\sin\theta_7 + C_1 = 0 \tag{5}$$

where

$$A_1 = 2r_7r_8 \tag{5a}$$

$$B_1 = 2r_7r_9 \tag{5b}$$

$$C_1 = r_7^2 + r_8^2 + r_9^2 - (r_5 + r_6)^2 \tag{5c}$$

By solving Eq. (5), the angular position of the handle, θ_7, is obtained as

$$\theta_7 = 2\tan^{-1}\left(\frac{-B_1 \pm \sqrt{A_1^2 + B_1^2 - C_1^2}}{C_1 - A_1}\right) \tag{6}$$

From Eqs. (4a) and (4b) and Fig. 6(a), the angles γ_1 and θ_4 can be expressed as

$$\gamma_1 = -\theta_5 = -\tan^{-1}\left(\frac{r_7\sin\theta_7 + r_9}{r_7\cos\theta_7 + r_8}\right) \tag{7}$$

$$\theta_4 = \alpha - \gamma_1 \tag{8}$$

From Fig. 6(a), the angle ξ_1 can be derived from the below equations

$$\tan(\pi - \xi_1) = \frac{r_4\sin\theta_4}{r_1 + r_4\cos\theta_4} = \frac{r_4\sin(\alpha - \gamma_1)}{r_1 + r_4\cos(\alpha - \gamma_1)} \tag{9}$$

$$\xi_1 = \pi - \tan^{-1}\frac{r_4\sin(\alpha - \gamma_1)}{r_1 + r_4\cos(\alpha - \gamma_1)} \tag{10}$$

From triangle $\Delta a_0b_0b_1$ and the law of cosines, the relationship can be derived as

$$\ell_1^2 = r_1^2 + r_4^2 - 2r_1r_4\cos(\pi - \alpha + \gamma_1) \tag{11}$$

where $\ell_1 = \overline{a_0b_1}$. Similarly, from triangle $\Delta a_0a_1b_1$ and the law of cosines, the relationship can be derived as

$$r_3^2 = r_2^2 + \ell_1^2 - 2r_2\ell_1\cos\eta_1 \tag{12}$$

From Eq. (12), the angle η_1 can be expressed as

$$\eta_1 = \cos^{-1}\frac{r_2^2 + \ell_1^2 - r_3^2}{2r_2\ell_1} \tag{13}$$

Furthermore, from Eqs. (10) and (13), the angle δ_1 can be obtained as

$$\delta_1 = \eta_1 - \xi_1 \tag{14}$$

When the foot support link is at the rear end **P2** of the pedal trajectory in Fig. 2, the difference between the position angles of vectors $\vec{r}_5$ and $\vec{r}_6$ is 180 degrees (as shown in Fig. 5), i.e. $\theta_6 = \theta_5 - \pi$. Rearranging Eqs. (3a) and (3b) yields

Copyright © TAETI

$$(r_5 - r_6)\cos\theta_5 = r_7\cos\theta_7 + r_8 \tag{15a}$$

$$(r_5 - r_6)\sin\theta_5 = r_7\sin\theta_7 + r_9 \tag{15b}$$

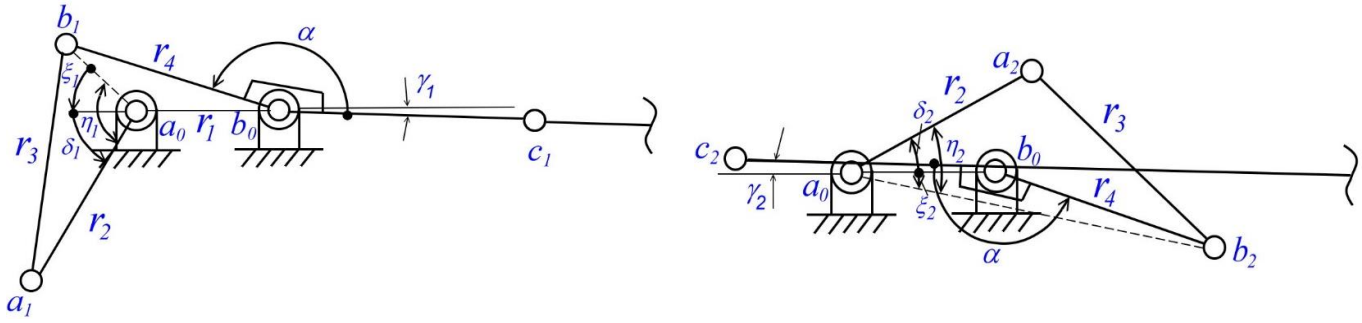

(a) Pedal at front end (b)Pedal at rear end

Fig. 6 Motion geometry on extreme positions

Squaring Eqs. (15a) and (15b) and adding them together, it yields

$$A_2\cos\theta_7 + B_2\sin\theta_7 + C_2 = 0 \tag{16}$$

where

$$A_2 = 2r_7r_8 \tag{16a}$$

$$B_2 = 2r_7r_9 \tag{16b}$$

$$C_2 = r_7^2 + r_8^2 + r_9^2 - (r_5 - r_6)^2 \tag{16c}$$

By solving Eq. (16), the angular position of the handle, θ_7, is obtained as

$$\theta_7 = 2\tan^{-1}\left(\frac{-B_2 \pm \sqrt{A_2^{\,2} + B_2^{\,2} - C_2^{\,2}}}{C_2 - A_2}\right) \tag{17}$$

From Eqs. (15a) and (15b) and Fig. 6(b), the angles γ_2 and θ_4 can be expressed as

$$\gamma_2 = \pi - \theta_5 = \pi - \tan^{-1}\left(\frac{-r_7\sin\theta_7 - r_9}{-r_7\cos\theta_7 - r_8}\right) \tag{18}$$

$$\theta_4 = \alpha - \gamma_2 - \pi \tag{19}$$

From Fig. 6(b), the angle ξ_2 can be derived from the equations below

$$\tan\xi_2 = -\frac{r_4\sin\theta_4}{r_1 + r_4\cos\theta_4} = -\frac{r_4\sin(\alpha - \gamma_2 - \pi)}{r_1 + r_4\cos(\alpha - \gamma_2 - \pi)} \tag{20}$$

$$\xi_2 = -\tan^{-1}\frac{r_4\sin(\alpha - \gamma_2 - \pi)}{r_1 + r_4\cos(\alpha - \gamma_2 - \pi)} \tag{21}$$

From triangle $\Delta a_0b_0b_2$ and the law of cosines, the relationship can be derived as

$$\ell_2^2 = r_1^2 + r_4^2 - 2r_1r_4\cos(\alpha - \gamma_2) \tag{22}$$

where $\ell_2 = \overline{a_0b_2}$. From triangle $\Delta a_0a_2b_2$ and the law of cosines, the relationship can be derived as

$$r_3^2 = r_2^2 + \ell_2^2 - 2r_2\ell_2\cos\eta_2 \tag{23}$$

Copyright © TAETI

From Eq. (23), the angle η_2 can be expressed as

$$\eta_2 = \cos^{-1} \frac{r_2^2 + \ell_2^2 - r_3^2}{2 r_2 \ell_2} \tag{24}$$

Therefore, from Eqs. (21) and (24), the angle δ_2 can be obtained as

$$\delta_2 = \eta_2 - \xi_2 \tag{25}$$

Assume that ϕ_{12} is the angular displacement of the flywheel as the pedal trajectory changes from the front end **P1** to the rear end **P2**, and ϕ_{21} from the rear end **P2** to the front end **P1**. The summation of these two angles is 360 degrees, that is

$$\phi_{12} + \phi_{21} = 2\pi \tag{26}$$

Then the rotation angles of the two strokes of the foot trajectory between two extreme positions can be expressed as:

$$\phi_{12} = \pi + \delta_1 - \delta_2 \tag{27}$$

$$\phi_{21} = 2\pi + \phi_{12} \tag{28}$$

Time ratio (TR) is the ratio of time required for the slow stroke to the time required for the quick stroke. If the flywheel runs at constant velocity, the time ratio TR can be expressed as:

$$TR = \frac{\phi_{12}}{\phi_{21}} \tag{29}$$

4. Kinematic analysis

When the dimensions of the elliptical exerciser linkage are known, the complete position analysis and pedal trajectory can be derived and calculated. By expressing the Eq. (1) into *X* and *Y* scalar component equations and rearranging them, the equations become

$$r_3 \cos\theta_3 = r_4 \cos\theta_4 + r_1 - r_2 \cos\theta_2 \tag{30a}$$

$$r_3 \sin\theta_3 = r_4 \sin\theta_4 - r_2 \sin\theta_2 \tag{30b}$$

Squaring Eqs. (30a) and (30b) and adding them together, it yields

$$A_3 \cos\theta_4 + B_3 \sin\theta_4 + C_3 = 0 \tag{31}$$

where

$$A_3 = 2r_4(r_1 - r_2 \cos\theta_2) \tag{31a}$$

$$B_3 = -2r_2 r_4 \sin\theta_2 \tag{31b}$$

$$C_3 = r_4^2 - r_3^2 + r_2^2 + r_1^2 - 2r_1 r_2 \cos\theta_2 \tag{31c}$$

By solving Eq. (31), the angular position of the bell crank, θ_4, is obtained as

$$\theta_4 = 2\tan^{-1}\left(\frac{-B_3 \pm \sqrt{A_3^2 + B_3^2 - C_3^2}}{C_3 - A_3}\right) \tag{32}$$

From Eqs. (30a) and (30b), the angular position of the connecting link, θ_3, is obtained as

Copyright © TAETI

$$\theta_3 = \tan^{-1}\frac{r_4\sin\theta_4 - r_2\sin\theta_2}{r_4\cos\theta_4 + r_1 - r_2\cos\theta_2} \tag{33}$$

θ_5 can be calculated by using $\theta_5 = \theta_4 - \alpha$. Rearranging Eqs. (3a) and (3b), the equations become

$$r_6\cos\theta_6 = r_7\cos\theta_7 + r_8 - r_5\cos\theta_5 \tag{34a}$$

$$r_6\sin\theta_6 = r_7\sin\theta_7 + r_9 - r_5\sin\theta_5 \tag{34b}$$

Squaring Eqs. (34a) and (34b) and adding them together, it yields

$$A_4\cos\theta_7 + B_4\sin\theta_7 + C_4 = 0 \tag{35}$$

Where

$$A_4 = 2r_7(r_8 - r_5\cos\theta_5) \tag{35a}$$

$$B_4 = 2r_7(r_9 - r_5\sin\theta_5) \tag{35b}$$

$$C_4 = r_5^2 - r_6^2 + r_7^2 + r_8^2 + r_9^2 - 2r_5r_8\cos\theta_5 - 2r_5r_9\sin\theta_5 \tag{35c}$$

By solving Eq. (35), the angular position of the handle, θ_7, is obtained as

$$\theta_7 = 2\tan^{-1}\left(\frac{-B_4 \pm \sqrt{A_4^{\,2} + B_4^{\,2} - C^{\,2}}}{C_4 - A_4}\right) \tag{36}$$

From Eqs. (34a) and (34b), the angular position of the foot support link, θ_6, is obtained as

$$\theta_6 = \tan^{-1}\frac{r_7\sin\theta_7 + r_9 - r_5\sin\theta_5}{r_7\cos\theta_7 + r_9 - r_5\cos\theta_5} \tag{37}$$

Therefore, the pedal position (x_p, y_p) with respect to the fixed pivot of the bell crank can be expressed as

$$x_p = r_5\cos\theta_5 + r_{6g}\cos\theta_6 \tag{38a}$$

$$y_p = r_5\sin\theta_5 + r_{6g}\sin\theta_6 \tag{38b}$$

5. Design Example

A design example is presented in this section for explaining the design procedure of the proposed innovative mechanism. Assume that the design parameters, r_5, r_6, r_7, r_8 and r_9 are 28.0cm, 134.0cm, 93.0cm, 143.0cm and 82.0cm, respectively. The time ratio TR of this mechanism is 1.30. When the foot support link is at the front end of the pedal trajectory, the position angles of vectors $\vec{r}_5$ and $\vec{r}_6$ are the same. Therefore, from Eqs. (6) and (7), the angles θ_7 and γ_1 are calculated as $\theta_7 = -78.37^o$ and $\gamma_1 = 3.22^o$, respectively. When the foot support link is at the rear end of the pedal trajectory, the difference between the position angles of vectors $\vec{r}_5$ and $\vec{r}_6$ is 180 degrees. Therefore, from Eqs. (17) and (18), the angles θ_7 and γ_2 are calculated as $\theta_7 = -113.48^o$ and $\gamma_2 = 1.78^o$. Moreover, by substituting TR into Eq. (29) and solving with Eq. (26) simultaneously, it yields $\varphi_{12} = 156.52^o$ and $\varphi_{21} = 203.48^o$.

After substitute the above parameters into Eqs. (10), (11), (13), (14), (21), (22), (24), (25), and (27), there are nine equations and thirteen unknowns ($r_1, r_2, r_3, r_4, \alpha, \delta_1, \delta_2, \xi_1, \xi_2, \ell_1, \ell_2, \eta_1, \eta_2$). Therefore, four of the unknowns can be freely specified and these parameters are selected as $\delta_1 = 60^o$, $\alpha = 175^o$, $r_1 = 10.0$ cm and $r_4 = 28.0$ cm. As a result, $\xi_1 = 12.73^o$, $\xi_2 = 5.0^o$, $\ell_1 = 18.159$ cm and $\ell_2 = 37.948$ cm can be solved by substituting the parameters into Eqs. (10)-(11) and (21)-(22).

Copyright © TAETI

Furthermore, $\delta_2 = 36.5^o$, $\eta_1 = 73.73^o$ and $\eta_2 = 41.52^o$ can be solved by substituting the parameters into Eqs. (27), (14) and (25). Finally, $r_2 = 24.15$ cm and $r_3 = 25.521$ cm can be solved simultaneously by substituting the parameters into Eqs. (12) and (23). The dimensions of the elliptical exerciser studied in this paper are listed in Table 1.

6. Results and Discussion

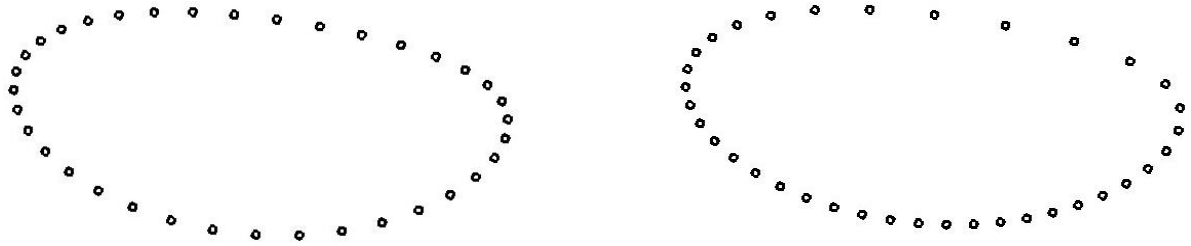

(a) Conventional design (b) Proposed design

Fig. 7 Pedal trajectory of conventional and proposed design

By way of using the vector-loop method and the kinematic analysis, motion simulation of the pedal trajectory is calculated and drawn to validate the design of the proposed innovative mechanism. The pedal trajectories of a conventional design and the proposed design are shown in Fig. 7. There is an interval of 10 degrees of flywheel rotation between two adjacent points on the pedal trajectory. In Fig. 7(a), the distance between the adjacent points near the front and rear end of the conventional pedal trajectory is closer and that near the midpoint on the supporting and striding travels is farther. In Fig. 7(b), the distance between the adjacent points at the bottom of the pedal trajectory of the proposed design is closer and that on the top of pedal trajectory is farther. If the flywheel runs at a constant speed, the speed of the foot near the front and rear ends of the conventional pedal trajectory is slower and that near the midpoint on the supporting and striding travels is faster. However, the speed of the foot of the proposed design on the supporting travel is slower than that on the striding travel.

Table 1 Dimensions of elliptical exerciser

Length	cm
r_1	10.00
r_2	24.15
r_3	25.521
r_4	28.00
r_5	28.00
r_6	134.00
r_7	93.00
r_8	143.00
r_9	82.00
Angle	degree
α	175.0^o
δ_1	60.0^o
δ_2	36.5^o
η_1	73.73^o
η_2	41.52^o

The distance between the adjacent points on pedal trajectory within an interval of 10 degrees of flywheel rotation is shown in Fig. 8. When the flywheel is at about 170^o and 350^o of the conventional design, i.e. at the front and rear end of the trajectory, the distance is about 2 cm. The shortest distance means the slowest speed. On the contrary, when the flywheel is at about 70^o and 270^o, i.e. in the middle of the supporting and striding travels, the distance is about 5 cm. The longest distance means the fastest speed.

Copyright © TAETI

However, when the flywheel is at 225° of the proposed design, i.e. at the rear end of the pedal trajectory, the distance is about 2 cm. The shortest distance means the slowest speed. When the flywheel is between 0° and 225°, i.e. at the bottom part of the pedal trajectory, the distance is kept between 2 and 3 cm. On the contrary, when the flywheel is at about 300°, i.e. in the middle of the striding travel, the distance is about 8 cm. The longest distance means the fastest speed. That means the average speed within striding travel is faster than that within the supporting travel. Therefore, by way of using the quick-return effect, the timing of the pedal trajectory in this innovative design is more similar to which in the real jogging and meets the principles of ergonomics. When using this proposed elliptical exerciser, the user can shift his body weight from one leg to the other before each of his legs stretch to its extreme positions. This motion pattern prevents the user from muscle sore and pain. Finally, by way of using a 3D modeling software, SolidWorks, the model of this innovative elliptical exerciser is constructed and shown in Fig. 9. Thus, the proposed innovative elliptical exerciser can be further fabricated, assembled, and tested.

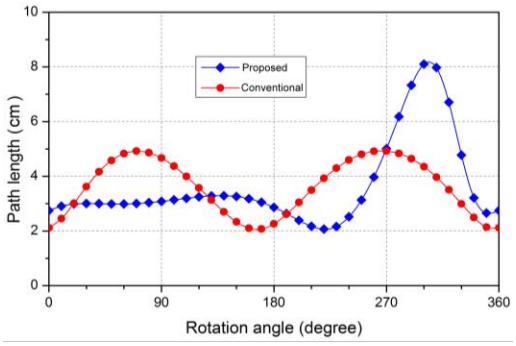

Fig. 8 Path length

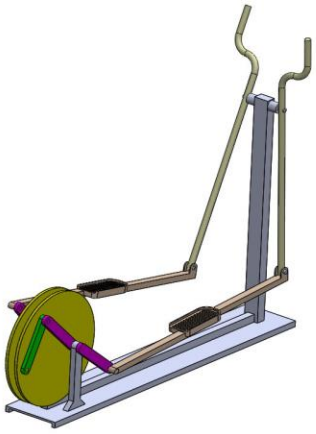

Fig. 9 CAD model of the innovative elliptical exerciser

7. Conclusions

This study proposes and investigates an innovative elliptical exerciser with quick-return effect that mimics the timing of the foot trajectory while jogging. At first, the innovative mechanism of the elliptical exerciser with quick-return effect is proposed and analysed kinematically using the vector-loop method and motion geometry. A design example is presented for explaining the design procedure of the proposed innovative design. Then, the pedal trajectory and the path length of the innovative elliptical exerciser are simulated. From the results, when the pedal of the elliptical exerciser is at the bottom part of pedal trajectory, the path distance keeps between 2 and 3 cm. On the contrary, when the pedal is in the middle of the striding travel, the path distance is about 8 cm. The longest path distance means the fastest speed. That means the average speed within striding travel is faster than that within the supporting travel. Therefore, by way of using the quick-return effect, the timing of the pedal trajectory in this innovative design is more similar to which in the real jogging and meets the principles of ergonomics. Finally, by way of using a 3D modeling software, SolidWorks, the model of this innovative elliptical exerciser is constructed for further development.

Copyright © TAETI

Acknowledgement

The authors are thankful to the Ministry of Science and Technology of the Republic of China for sponsoring this research under grant MOST 106-2221-E-168-003.

References

[1] G. H. Martin, Kinematics and dynamics of machines, 2nd ed., New York: McGraw-Hill, 1982.
[2] H. S. Yan, Mechanisms: theory and applications, New York: McGraw-Hill, 2016.
[3] S. N. Dwivedi, "Application of a Whitworth quick return mechanism for high velocity impacting press," Mechanism and Machine Theory, vol. 19, no. 1, pp. 51-59, January 1984.
[4] F. O. Suareo and K. C. Gupta, "Design of quick-returning R-S-S-R mechanisms," Journal of Mechanisms, Transmissions, and Automation in Design, vol. 110, no. 4, pp. 423-428, December 1988.
[5] D. G. Beale and R. A. Scott, "The stability and response of a flexible rod in a quick return mechanism," Journal of Sound and Vibration, vol. 141, no. 2, pp. 277-289, September 1990.
[6] R. F. Fung and K. W. Chen, "Constant speed control of the quick return mechanism driven by a DC motor," JSME International Journal, Series C, vol. 40, no. 3, pp. 454-461, September 1997.
[7] R. F. Fung and F. Y. Lee, "Dynamic analysis of the flexible rod of a quick-return mechanism with time-dependent coefficients by the finite element method," Journal of Sound and Vibration, vol. 202, no. 2, pp. 187-201, May 1997.
[8] R. F. Fung and K. W. Chen, "Vibration suppression and motion control of a non-linearly coupled flexible quick-return mechanism driven by a PM synchronous servo motor," Journal of Sound and Vibration, vol. 212, no. 4, pp. 721-742, May 1998.
[9] F. J. Lin and R. J. Wai, "A hybrid computed torque controller using fuzzy neural network for motor-quick-return servo mechanism," IEEE/ASME Transactions on Mechatronics, vol. 6, no. 1, pp. 75-89, March 2001.
[10] F. J. Lin and R. J. Wai, "Adaptive and fuzzy neural network sliding-mode controllers for motor-quick-return servomechanism," Mechatronics, vol. 13, no. 5, pp. 477-506, June 2003.
[11] J. L. Ha, J. R. Chang, and R. F. Fung, "Dynamic analyses of a flexible quick-return mechanism by the fixed and variable finite-difference grids," Journal of Sound and Vibration, vol. 297, no. 1-2, pp. 365-381, October 2006.
[12] J. R. Chang, "Coupling effect of flexible geared rotor on quick-return mechanism undergoing three-dimensional vibration," Journal of Sound and Vibration, vol. 300, no. 1-2, pp. 139-159, February 2007.
[13] W. H. Hsieh and C. H. Tsai, "A study on a novel quick return mechanism," Transactions of the Canadian Society for Mechanical Engineering, vol. 33, no. 3, pp.139-152, September 2009.
[14] J. H. Shyu, C. K. Chen, C. C. Yu, and Y. J. Luo, "Research and development of an adjustable elliptical exerciser," Advanced Materials Research, vols. 308-310, pp. 2078-2083, August 2011.
[15] C. A. Nelson and J. M. Burnfield, "Improved elliptical trainer biomechanics using a modified Cardan gear," Proc. ASME 36th Mechanisms and Robotics Conference, vol. 4, 2012, pp. 35-42.
[16] J. P. Porcari, J. M. Zedaker, L. Naser, and M. Miller, "Evaluation of an elliptical exerciser in comparison to treadmill walking and running, stationary cycling, and stepping," Medicine & Science in Sports & Exercise, vol. 30, no. 5, p. 168, May 1998.
[17] J. Porcari, C. Foster, and P. Schneider, "Exercise response to elliptical trainers," Fitness Management, pp. 1-3, August 2000.
[18] H. Sozen, "Comparison of muscle activation during elliptical trainer, treadmill and bike exercise," Biology of Sport, vol. 27, no. 3, pp. 203-206, August 2010.
[19] L. Louie and Y. T. Lam, "A comparison on selected physiological variables between two models of elliptical cross trainers," Asian Journal of Physical Education & Recreation, vol. 17, no. 1, pp. 91-103, April 2011.

Copyright © TAETI